

Fig. 1. Band offsets between silicon and different high-k materials. Ultra-thin high-k materials could promote the formation of quantum wells by taking advantage of these offsets. Resonant tunneling could be promoted for these materials.

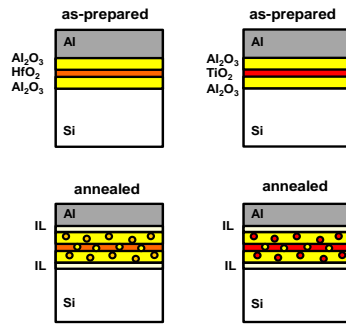


Fig. 2. a) Schematic of the resulting as-prepared MIIS devices. b) PMA would promote generation of interfacial layers (IL) and out-diffusion of elements in stacked oxides.

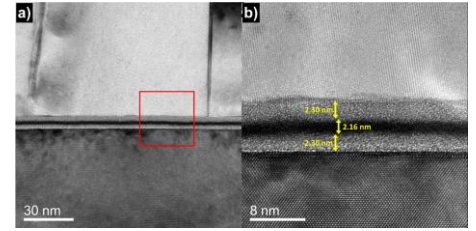


Fig. 3. a) TEM image of the as-prepared AHA structure, notice the different grains visible in the aluminum top layer. b) HR-TEM image of the region highlighted in (a) with measurements of the amorphous oxide layers

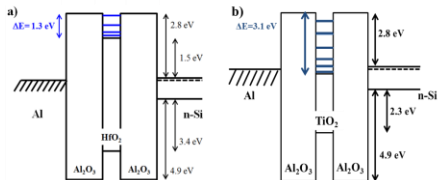


Fig. 4 a) Ideal band diagram for the as-prepared $\text{Al}_2\text{O}_3/\text{HfO}_2/\text{Al}_2\text{O}_3$. 4 discrete energy levels are found due to a highly confined structure. These discrete energy levels promote RT b) Ideal band diagram for the as-prepared $\text{Al}_2\text{O}_3/\text{TiO}_2/\text{Al}_2\text{O}_3$. Here, 6 discrete energy levels are found.

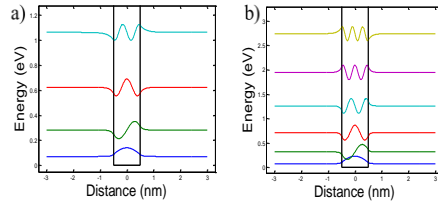


Fig. 5 a) Solution of the Schrödinger equation for a QW of 1.3 eV, corresponding to the as-prepared $\text{Al}_2\text{O}_3/\text{HfO}_2/\text{Al}_2\text{O}_3$ device. b) Solution of the Schrödinger equation for a QW of 3.1 eV, corresponding to the as-prepared $\text{Al}_2\text{O}_3/\text{TiO}_2/\text{Al}_2\text{O}_3$ device.

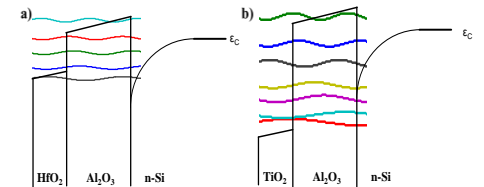


Fig. 6. a) Solution of the Schrödinger equation for a positive bias for the $\text{Al}_2\text{O}_3/\text{HfO}_2/\text{Al}_2\text{O}_3$ device. 4 energy levels are bounded. b) Solution of the Schrödinger equation for positive bias for the $\text{Al}_2\text{O}_3/\text{TiO}_2/\text{Al}_2\text{O}_3$ device. 6 energy levels are bounded.

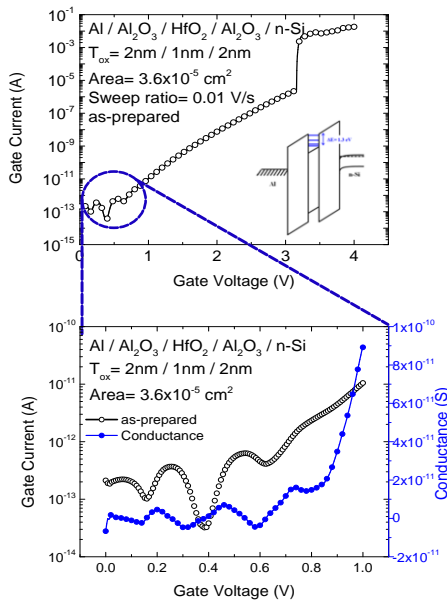


Fig. 7. a) I_g - V_g characteristics of the as-prepared AHA structure. At $V_g < 1\text{V}$, 3 NDR zones are observed related to 3 quantized energy levels in the CB of HfO_2 . The inset shows an ideal energy band diagram for this MIIS structure along with some quantized energy levels in the CB of HfO_2 . b) Amplified view of the data already presented and its conductance characteristics showing different slopes to each NDR zone.

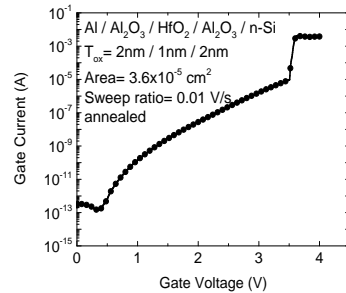


Fig. 8. a) I-V characteristics of the annealed AHA structure. Formation of multiple NDR zones is lost, only a faint decrease in current with applied bias is observed at $V < 0.5\text{V}$.

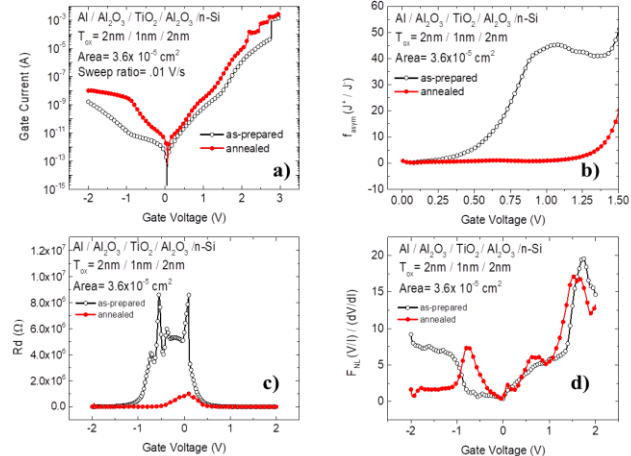


Fig. 9. a) I-V characteristics of the $\text{Al}_2\text{O}_3/\text{TiO}_2/\text{Al}_2\text{O}_3$ devices. No evident NDR zones are observed. b) Asymmetry for the ATA devices, as seen, the as-prepared sample presents a higher asymmetry, related to a higher RT. c) Dynamic resistance for MIIS devices. d) Non-linearity for ATA devices, a value of 3 denotes resonance, in this case, the as-prepared structure presents a maximum value of around 20.